B. Equivalent Circuit Analysis

In order to understand the operation mechanism of the NRD guide circulator and develop a design theory, analysis is made based on an equivalent circuit representation. In general, the circulator can be represented in terms of a three-by-three scattering matrix [11], [12]. Each matrix element can be determined, as discussed by Goebel and Schieblich [12], if the resonant frequencies of the clockwise and counterclockwise rotating modes in the dc biased ferrite resonator are calculated or measured. In addition, the effect of discontinuity between the dielectric strip and the ferrite resonator can be taken into account by introducing a small segment of the dielectric strip of normal cross-sectional size between each dielectric strip and the ferrite resonator. Typically, the length of such a small segment was found to be 0.7 mm.

Now, characteristics of the NRD guide circulator can be simulated in terms of various given parameters. Among them, the parameters which have to be measured are only the resonant frequencies of the clockwise and counterclockwise rotating modes in the ferrite resonator and the length of the small dielectric segment.

The insertion loss and the isolation are calculated at 50 GHz for the circulator with the dielectric strip 2.4 mm in width and the half-wavelength steps 1.8 mm in width, and are plotted with solid curves in Fig. 7, in comparison with the results of measurement. Agreement between calculation and measurements is excellent, although the step width assumed in theory is slightly different from that used in measurement. This discrepancy between theory and measurement seems to be caused by unavoidable fabrication error related to the insertion of the mode suppressors and loss in the ferrite material. Nevertheless, the equivalent circuit analysis is very useful, since it can predict the optimum width of the half-wavelength steps as well as the performance characteristics of the circulator.

V. Conclusion

A high-performance NRD guide circulator has been constructed by incorporating mode suppressors and half-wavelength steps on the dielectric strips. The fabricated circulator has an insertion loss less than 0.3 dB and a 20 dB isolation bandwidth of about 2.6 GHz. Equivalent circuit analysis of the circulator has proved to be especially useful for predicting the optimum step width needed for band widening the circulator.

References

[1] W. S. Piotrowski and J. E. Raue, "Low-loss broad-band EHF circulator," *IEEE Trans. Microwave Theory Tech.*, vol. MTT-24, pp. 863–866, Nov. 1976.

[2] K. Chang *et al.*, "*W*-band (75–110 GHz) microstrip components," *IEEE Trans. Microwave Theory Tech.*, vol. MTT-33, pp. 1375–1382, Dec. 1985.

[3] U. Goebel and C. Schieblich, "Broadband fin-line circulators," in *1982 IEEE MTT-S Int. Microwave Symp. Dig.*, June 1982, pp. 249–251.

[4] R. A. Stern and R. W. Babbitt, "Dielectric waveguide circulator," *Int. J. Infrared and Millimeter Waves*, vol. 3, no. 1, pp. 11–18, Jan. 1982.

[5] T. Yoneyama and S. Nishida, "Nonradiative dielectric waveguide for millimeter-wave integrated circuits," *IEEE Trans. Microwave Theory Tech.*, vol. MTT-29, pp. 1188–1192, Nov. 1981.

[6] L. E. Davis and S. R. Longley, "*E*-plane 3-port *X*-band waveguide circulators," *IEEE Trans. Microwave Theory Tech.*, vol. MTT-11, pp. 443–445, Sept. 1963.

[7] B. Owen, "The identification of modal resonances in ferrite loaded waveguide Y-junctions and their adjustment for circulation," *Bell Syst. Tech. J.*, vol. 51, no. 3, pp. 595–627, Mar. 1972.

[8] C. E. Fay and R. L. Comstock, "Operation of the ferrite junction circulator," *IEEE Trans. Microwave Theory Tech.*, vol. MTT-13, pp. 15–27, Jan. 1965.

[9] L. K. Anderson, "An analysis of broadband circulators with external tuning elements," *IEEE Trans. Microwave Theory Tech.*, vol. MTT-15, pp. 42–47, Jan. 1967.

[10] Y. Akaiwa, "Bandwidth enlargement of a millimeter-wave Y circulator with half-wavelength line resonators," *IEEE Trans. Microwave Theory Tech.*, vol. MTT-22, pp. 1283–1286, Dec. 1974.

[11] J Helszajn, *Nonreciprocal Microwave Junctions and Circulators*. New York: Wiley, 1975.

[12] U. Goebel and C. Schieblich, "A unified equivalent circuit representation for *H*- and *E*-plane junction circulators," in *Proc 13th Eur. Microwave Conf* (Nuernberg), 1983, pp. 803–808.

[13] T. Yoneyama *et al.*, "Analysis and measurements of nonradiative dielectric waveguide bends," *IEEE Trans Microwave Theory Tech*, vol. MTT-34, pp 876–882, Aug. 1986.

[14] T Yoneyama, "Nonradiative dielectric waveguide," in *Infrared and Millimeter waves*, vol. 11, K. J. Button, Ed. New York: Academic Press, 1984, pp. 61–98.

Thick Circular Iris in a TE_{11} Mode Circular Waveguide

ROBERT W. SCHARSTEIN, MEMBER, IEEE, AND ARLON T. ADAMS, SENIOR MEMBER, IEEE

***Abstract*—The TE_{11} mode excitation of a concentric circular iris of finite thickness in a circular waveguide is analyzed by Galerkin's method with even and odd excitation. Agreement between calculated and measured dominant mode scattering parameters is generally within experimental accuracy.**

I. Introduction

The thick circular iris of Fig. 1 has an aperture of radius b, is of longitudinal thickness T, and is concentrically located in a circular waveguide of radius a. There is a transverse plane of symmetry through the center of the iris. Employing superposition, excitation of the iris from the left is equivalent to in-phase (even) excitation from both sides plus out-of-phase (odd) excitation from both sides [1, p. 354]. According to image theory, a shorting perfect magnetic conductor (tangential $\bar{H} = 0$ or open circuit) placed at the symmetry plane in the center of the thick iris and excited from the left (Fig. 2) is equivalent to the even excitation case as far as the total fields to the left of the plane are concerned. Similarly, a perfect electric conductor (tangential $\bar{E} = 0$ or short circuit) at the symmetry plane produces the same total fields to the left of the plane as the odd excitation case. Each of these problems is solved separately with the desired TE_{11} mode incident from the left. The total fields everywhere to the left of the symmetry plane in the thick iris problem are then given by the sum of the separate fields:

$$(\bar{E}, \bar{H})_{\text{total}} = \frac{1}{2}(\bar{E}, \bar{H})_{\text{even}} + \frac{1}{2}(\bar{E}, \bar{H})_{\text{odd}}. \tag{1}$$

II. Analysis

The TE_{11} mode excitation of the infinitesimally thin circular iris is treated in [2]. Approximating the transverse electric field in the aperture ($z = 0$) plane by a finite set of M TE_{1m} modes and N TM_{1m} modes of waveguide (b)

$$\bar{E}_{\text{aper}}(\bar{\rho}) = \sum_{l=1}^{M} \tilde{V}_l^h \tilde{\bar{e}}_l^h(\bar{\rho}) + \sum_{l=1}^{N} \tilde{V}_l^e \tilde{\bar{e}}_l^e(\bar{\rho}), \qquad \bar{\rho} \in S \tag{2}$$

Manuscript received December 14, 1987; revised May 28, 1988.

R. W. Scharstein is with the SENSIS Corporation, DeWitt, NY 13214

A. T. Adams is with the Department of Electrical and Computer Engineering, Syracuse University, Syracuse, NY 13210.

IEEE Log Number 8823256.

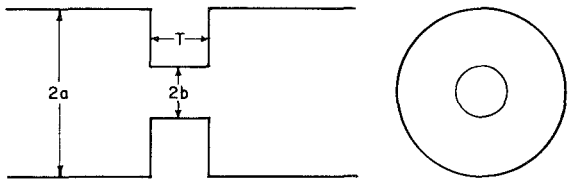

Fig. 1. Thick circular iris in circular waveguide.

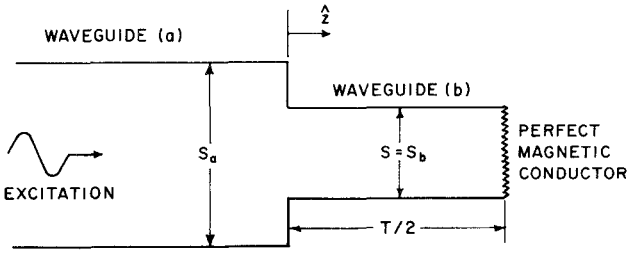

Fig. 2. Junction geometry for even excitation problem.

in Galerkin's method [3] yields the matrix equation

$$(\bar{\bar{Y}}^a + \bar{\bar{Y}}^b)\,\tilde{\bar{V}} = \bar{I}^a \tag{3}$$

for the column vector of unknown coefficients of $L = N + M$ aperture modes, or aperture voltages $\tilde{\bar{V}}$. The (k, l)th element of the left side aperture admittance matrix is

$$Y^a_{kl} = \sum_{m=1}^{\infty} y_m \langle \bar{e}_m, \tilde{\bar{e}}_k \rangle_{S_b} \langle \tilde{\bar{e}}_l, \bar{e}_m \rangle_{S_b} \tag{4}$$

and the kth element of the column vector of current excitations is

$$I^a_k = 2\, y^h_1 \langle \bar{e}^h_1, \tilde{\bar{e}}_k \rangle_{S_b} \tag{5}$$

where y_m is the mth modal admittance and $\bar{e}_m$ is the mth normalized transverse electric field modal function. The Poisson brackets denote the inner product between waveguide (a) and aperture modal functions:

$$\langle \bar{e}_m, \tilde{\bar{e}}_k \rangle_{S_b} = \iint_{S_b} \bar{e}_m \cdot \tilde{\bar{e}}^*_k \, ds. \tag{6}$$

The right side aperture admittance matrix has elements

$$Y^b_{kl} = \sum_{n=1}^{\infty} \tilde{y}^{\text{eff}}_n \langle \tilde{\bar{e}}_n, \tilde{\bar{e}}_k \rangle_{S_b} \langle \tilde{\bar{e}}_l, \tilde{\bar{e}}_n \rangle_{S_b} \tag{7}$$

but due to mode orthogonality reduces to the diagonal matrix

$$Y^b_{kl} = \tilde{y}^{\text{eff}}_k \delta_{kl}. \tag{8}$$

The notation used is a tilde $(\tilde{\ })$ for aperture quantities, which are also waveguide (b) quantities, and no superscript for waveguide (a) quantities. The effects of the shorting conductor placed a distance $T/2$ to the right of the aperture plane are accounted for by the resultant effective modal admittance of the waveguide,

$$\tilde{y}^{\text{eff}}_n = \begin{cases} \tilde{y}_n \tanh\left(\dfrac{\tilde{\gamma}_n T}{2}\right), & \text{even case} \\ \tilde{y}_n \coth\left(\dfrac{\tilde{\gamma}_n T}{2}\right), & \text{odd case} \end{cases} \tag{9}$$

where $\tilde{\gamma}_n$ is the propagation constant of the nth aperture mode. Note that for a lossless iris region, propagating iris modes ($\tilde{\gamma}_n = j\tilde{\beta}_n$) can experience the same internal resonance problem reported in [4] and [5]. This resonance occurs when the thickness T is an odd multiple of aperture guide half-wavelengths for the even excitation case and occurs when T is an integral number of aperture guide full wavelengths for the odd excitation case. As indicated by [4] and [5], a slight perturbation of dimensions or frequency or the addition of a small amount of dielectric loss alleviates this potential numerical difficulty.

TABLE I
CALCULATED AND MEASURED S PARAMETERS

Thickness T (inch)	REFLECTION COEFFICIENT S_{11}				TRANSMISSION COEFFICIENT S_{21}			
	Calculated		Measured		Calculated		Measured	
	Magnitude	Phase (°)	Magnitude	Phase (°)	Magnitude	Phase (°)	Magnitude	Phase (°)
0.005	0.867	149.8	0.855	150.5	0 498	59.8	0.465	56 8
0.008	0.874	150.4	0.866	151.7	0.485	60.4	0.451	59.3
0.050	0.934	155.7	0.927	155.3	0.356	65.7	0.330	62.6
0.100	0.966	158.6	0.956	158.1	0.260	68.6	0.240	65.1
0.200	0.990	161.0	0.981	160.6	0.144	71.0	0.134	67.1
0.500	1.000	162 0	0.993	161.1	0 027	72.0	0.026	69.0
1.000	1.000	162 0	0.995	161.5	0 002	72.0	0.002	70.1
3.000	1 000	162.0	0.993	160.6	0 000	75.7	0.000	-36.6

$a = 0.50175$ in; $b = 0.25$ in; $f = 9.0$ GHz.

TABLE II
CALCULATED AND MEASURED S PARAMETERS

Thickness T (inch)	REFLECTION COEFFICIENT S_{11}				TRANSMISSION COEFFICIENT S_{21}			
	Calculated		Measured		Calculated		Measured	
	Magnitude	Phase (°)	Magnitude	Phase (°)	Magnitude	Phase (°)	Magnitude	Phase (°)
0 005	0.331	108.7	0.319	115.2	0.943	18.7	0.924	17.7
0 008	0.344	109.1	0.335	117.1	0.939	19.1	0.919	18.2
0.050	0.488	113.2	0.476	115.2	0.873	23.2	0.852	21.9
0 100	0.622	116.8	0.610	118.3	0.783	26.8	0.759	25.1
0.200	0.806	122.0	0.803	123.4	0.593	32.0	0.575	30.0
0 500	0.977	127.4	0.982	127 6	0.211	37.4	0.207	34.5
1.000	0 999	128.1	1.006	128.5	0.034	38.1	0.035	36.1
3.000	1 000	128.2	1.006	128.0	0.000	38.1	0.000	47.2

$a = 0.50175$ in; $b = 0.25$ in; $f = 12$ GHz.

Any of the reciprocal two-port parameters and equivalent circuit elements are immediately calculable from the waveguide dominant mode voltage, which is the projection of the aperture field onto the TE_{11} waveguide mode:

$$V_1 = 1 + \Gamma = \sum_{l=1}^{M} \tilde{V}^h_l \langle \tilde{\bar{e}}^h_l, \bar{e}_1 \rangle_{S_b} + \sum_{l=1}^{N} \tilde{V}^e_l \langle \tilde{\bar{e}}^e_l, \bar{e}_1 \rangle_{S_b}. \tag{10}$$

The normalized input impedance measured at the iris face under either even or odd excitation is

$$Z_{\text{in}} = \frac{1+\Gamma}{1-\Gamma} = \frac{V_1}{2 - V_1}. \tag{11}$$

Scattering parameters are given by a standard transformation of the normalized impedance parameters, which are found via

$$Z_{11} + Z_{12} = Z_{\text{in}|_{\text{even}}} \qquad Z_{11} - Z_{12} = Z_{\text{in}|_{\text{odd}}} \tag{12}$$

III. RESULTS

A direct comparison [6] between calculated and measured TE_{11} mode S parameters for two iris radii (b) and eight iris thicknesses (T) at two frequencies is given in Tables I through IV. Measurements were made in air-filled brass circular waveguide with a mean diameter $2a = 1.0035$ in using the HP model 8409 B automatic network analyzer at X-band. A total of forty ($M = N = 20$) aperture modes were used in the Galerkin computations. The S parameter reference planes contain the iris faces.

TABLE III
CALCULATED AND MEASURED S PARAMETERS

Thickness T (inch)	REFLECTION COEFFICIENT S_{11}				TRANSMISSION COEFFICIENT S_{21}			
	Calculated		Measured		Calculated		Measured	
	Magni-tude	Phase (°)	Magni-tude	Phase (°)	Magni-tude	Phase (°)	Magni-tude	Phase (°)
0.005	0.199	100.8	0.194	101.0	0.980	10.8	0.961	11.0
0.008	0.205	100.8	0.200	100.6	0.979	10.8	0.956	11.1
0.050	0.272	99.3	0.271	99.6	0.962	9.3	0.935	9.4
0.100	0.337	97.0	0.335	96.6	0.941	7.0	0.911	6.6
0.200	0.453	92.4	0.451	92.4	0.892	2.4	0.854	2.3
0.500	0.706	82.0	0.701	81.7	0.708	-8.0	0.675	-6.9
1.000	0.901	73.4	0.897	73.0	0.434	-16.6	0.411	-14.9
3.000	0.999	68.7	0.998	67.4	0.052	-21.3	0.052	-20.0

$a = 0.50175$ in; $b = 0.375$ in; $f = 9.0$ GHz.

TABLE IV
CALCULATED AND MEASURED S PARAMETERS

Thickness T (inch)	REFLECTION COEFFICIENT S_{11}				TRANSMISSION COEFFICIENT S_{21}			
	Calculated		Measured		Calculated		Measured	
	Magni-tude	Phase (°)	Magni-tude	Phase (°)	Magni-tude	Phase (°)	Magni-tude	Phase (°)
0.005	0.006	89.3	0.006	79.5	1.000	-0.7	0.998	-0.6
0.008	0.005	88.5	0.008	28.7	1.000	-1.5	1.003	-1.2
0.050	0.014	-102.2	0.012	-59.7	1.000	-12.1	1.003	-11.7
0.100	0.033	-114.4	0.033	-99.8	0.999	-24.4	1.003	-25.4
0.200	0.056	-138.6	0.054	-129.3	0.998	-48.6	1.002	-49.1
0.500	0.040	150.8	0.051	161.1	0.999	-119.2	0.997	-120.3
1.000	0.067	-146.3	0.083	-141.3	0.998	123.7	0.993	121.6
3.000	0.010	-74.6	0.032	-131.1	1.000	15.4	0.991	11.6

$a = 0.50175$ in; $b = 0.375$ in; $f = 12.0$ GHz.

IV. CONCLUSIONS

The agreement between calculated and measured reflection and transmission coefficients is excellent, with larger errors or differences in the cases where the measured wave amplitude is small. Since the calculated and measured S parameters agree within experimental accuracy for several geometries and frequencies, and since the Galerkin analysis is equally valid over the entire range of geometries and frequencies under consideration, the differences are attributed to experimental error and dimensional tolerances of the iris samples. The changes in the reflection coefficient as a function of iris thickness indicate that the aperture fields also vary with iris thickness.

REFERENCES

[1] R. E. Collin, *Field Theory of Guided Waves*. New York: McGraw-Hill, 1960.

[2] R. W. Scharstein and A. T. Adams, "Galerkin solution for the thin circular iris in a TE_{11}-mode circular waveguide," *IEEE Trans Microwave Theory Tech.*, vol. 36, pp. 106–113, Jan. 1988.

[3] L. V. Kantorovich and V. I. Krylov, *Approximate Methods of Higher Analysis*. New York: Interscience, 1958, pp. 258–283.

[4] D. T. Auckland and R. F. Harrington, "Electromagnetic transmission through cascaded rectangular regions in a thick conducting screen," *Arch. Elek. Übertragung.*, Band 34, pp. 19–26, 1980.

[5] J. R. Mautz and R. F. Harrington, "*H*-field, *E*-field, and combined-field solutions for conducting bodies of revolution," *Arch. Elek. Übertragung.*, Band 32, pp. 159–164, 1978.

[6] R. W. Scharstein, "Electromagnetic analysis of waveguide junctions and irises using Galerkin's method," Ph.D. dissertation, Syracuse University, Syracuse, NY, 1986.

A Novel Type of Waveguide Polarizer with Large Cross-Polar Bandwidth

ERIK LIER, MEMBER, IEEE, AND TOR SCHAUG-PETTERSEN

Abstract—**In this paper a new wide-band quarter-wave polarizer is presented having a rectangular cross section, where all four walls are loaded with a dielectric or artificial dielectric. A much larger bandwidth compared to existing polarizers can be obtained without increasing the insertion loss. A polarizer has been measured with differential phase shift within $90° \pm 0.7°$ corresponding to 44 dB isolation, insertion loss below 0.06 dB, and return loss below −24 dB (VSWR < 1.13) over the frequency band 10.95 to 14.50 GHz.**

I. INTRODUCTION

Quarter-wave polarizers (transducers) in waveguide technology for transformation between linear and circular polarization may have various applications, such as in feed systems for the transmission and reception of circularly polarized satellite signals. They are also used in radar systems to separate one orthogonal polarization from the other. In [1], two quarter-wave polarizers were used to align the antenna to the correct linear polarization simply by rotating one of the polarizers. For that application an extremely wide band polarizer was needed.

Wide-band polarizers are known from the literature. Some of these apply a dielectric material in the waveguide, either a dielectric slab or a dielectric rod [2]. In [3] capacitive pins or irises were applied to provide the desired differential phase shift between the two orthogonal modes. A modification of this approach is described in [4], where two opposite walls in the quadratic waveguide are loaded with corrugations.

In the application described in [1] the isolation requirement could not be met by any of the polarizers known from the literature. A new polarizer approach was therefore developed and is presented in this paper.

II. POLARIZER APPROACH

A. Conventional Polarizer

The differential phase shift between the two orthogonal modes in conventional wide-band polarizers is illustrated in Fig. 1(b) as a function of ka ($k = 2\pi/\lambda$, where λ is the free-space wavelength, and a is some cross-sectional radius). Fig. 1(a) shows the dispersion characteristics for modes polarized in the x and y directions. We see that the curve for the differential phase shift has a minimum value $\Delta\varphi_m = \Delta\varphi(f_m) \propto |\beta_x(f_m) - \beta_y(f_m)|$, which should be close to 90° for single-band applications. This minimum occurs at the frequency f_m satisfying

$$\frac{\partial \beta_x}{\partial f} = \frac{\partial \beta_y}{\partial f} \tag{1a}$$

or

$$\frac{\partial}{\partial f}[\Delta\varphi(f)] = 0. \tag{1b}$$

In [5] an approximate mathematical model for this general polarizer approach is presented, where the differential phase shift is expressed as

$$\Delta\varphi = \Delta\varphi(f) = \frac{\Delta\varphi_m}{2}\left[\left(\frac{f^2 - f_c^2}{f_m^2 - f_c^2}\right)^{1/2} + \left(\frac{f_m^2 - f_c^2}{f^2 - f_c^2}\right)^{1/2}\right] \tag{2a}$$

$$= \frac{\Delta\varphi_m}{2}\left[(f/f_m)^{1/2} + (f_m/f)^{1/2}\right], \qquad f_c = 0 \tag{2b}$$

Manuscript received December 31, 1987; revised May 26, 1988. This work was supported by the Norwegian Telecommunications Administration.

The authors are with Satellite Systems, ELAB, N-7034 Trondheim NTH, Norway.

IEEE Log Number 8823260.